

Numerical Stability of Explicit Runge-Kutta Finite-Difference Schemes for the Nonlinear Schrödinger Equation

R. M. Caplan and R. Carretero-González

Nonlinear Dynamical System Group*, Computational Science Research Center, and
Department of Mathematics and Statistics, San Diego State University,
San Diego, California 92182-7720, USA

August 25, 2011

Abstract

Linearized numerical stability bounds for solving the nonlinear time-dependent Schrödinger equation (NLSE) using explicit finite-differencing are shown. The bounds are computed for the fourth-order Runge-Kutta scheme in time and both second-order and fourth-order central differencing in space. Results are given for Dirichlet, modulus-squared Dirichlet, Laplacian-zero, and periodic boundary conditions for one, two, and three dimensions. Our approach is to use standard Runge-Kutta linear stability theory, treating the nonlinearity of the NLSE as a constant. The required bounds on the eigenvalues of the scheme matrices are found analytically when possible, and otherwise estimated using the Gershgorin circle theorem.

1 Introduction

The nonlinear Schrödinger equation (NLSE) is used to model a wide variety of physical systems since it describes, to least nonlinear order, modulated wave propagation. [1]. The general form of the NLSE can be written as

$$i \frac{\partial \Psi}{\partial t} + a \nabla^2 \Psi - V(\mathbf{r}) \Psi + s |\Psi|^2 \Psi = 0, \quad (1)$$

where $\Psi \in \mathbb{C}$ is the value of the wavefunction, ∇^2 is the Laplacian operator, and where $a > 0$ and s are parameters defined by the system being modeled. $V(\mathbf{r})$ is an external potential term, which when included, makes Eq. (1) known as the Gross-Pitaevskii equation [2].

Often, efficient and easy-to-use numerical methods are employed to simulate the NLSE. One such method is the method of lines where the time-stepping and spatial differencing are treated independently. This transforms the partial differential equation (PDE) into a large number of coupled ordinary differential equations (ODEs). These ODEs can then be solved using a variety of numerical schemes, one of the most common being the fourth order Runge-Kutta (RK4) scheme [3]. Using the RK4 scheme with the NLSE produces a fully explicit scheme where each grid point at time t is only a function of values at time $t - k$ where k is the time-step. This simplifies computational implementations because no matrices are needed to be formed and stored, and no linear systems are needed to be solved (which in the nonlinear case also require a nonlinear iterative process).

One drawback to explicit schemes (such as the RK4) for PDEs is that they are conditionally stable. This means that there is an upper bound on the allowed size of the time-step which is dependent on the spatial-step size. If the time-step is larger than this bound, the scheme is unstable and diverges [4]. Although

*URL: <http://nlds.sdsu.edu>

rough estimates of the stability bound can be found through educated guess and check, for higher dimensional scenarios, as well as long and/or large simulations, a more refined and predictable stability bound is essential for efficient simulations.

In this paper, we formulate linearized stability bounds for simulating the NLSE with the RK4 scheme. The stability bounds depend on the specific spatial differencing scheme being used, as well as on the boundary conditions. We formulate the bounds for both second-order and fourth-order spatial differencing with a variety of boundary conditions (dirichlet, modulus-squared Dirichlet, Laplacian-zero, and periodic). Each analysis is done for one, two and three dimensions.

The paper is organized as follows. In Section 2 we review the basic RK4 stability properties and apply the results to the NLSE to formulate general stability bounds. Our basic procedure in finding the stability bounds and the linear algebra theorems that we utilize are also discussed. In Section 3 we summarize the forms of the boundary conditions we consider. Our main analysis begins in Section 4 with the one-dimensional NLSE. Linearized stability bounds are found for each scheme and boundary condition combination. In Sections 5 and 6, we use the same procedures to formulate the bounds for the two- and three-dimensional NLSE respectively. In Section 7, we conclude and summarize all the results from Sections 4, 5, and 6 into a concise reference.

2 Stability Theory

2.1 General Runge-Kutta Scheme Stability

Given an initial value problem of a set of linear first-order ODEs (or an explicit PDE finite-difference scheme), one can formulate the matrix notation

$$\frac{\partial \vec{\Psi}}{\partial t} = \mathcal{A} \vec{\Psi}, \quad (2)$$

where \mathcal{A} contains the coefficients of the right-hand-sides of the ODEs with boundary conditions (which in our case, includes the finite-difference stencils). We now define

$$\vec{p} = k \vec{\lambda}, \quad (3)$$

where k is the time-step size and $\vec{\lambda}$ are the eigenvalues of \mathcal{A} . In the case of a PDE, the eigenvalues of \mathcal{A} will have the spatial-step size (denoted h) included in them, as well as any parameters of the PDE. As shown in Ref. [5], for the fourth-order Runge-Kutta scheme, we define a vector $\vec{R}(\vec{p})$ whose elements are the polynomials

$$R(p) = 1 + p + \frac{p^2}{2} + \frac{p^3}{6} + \frac{p^4}{24}. \quad (4)$$

Inserting Eq. (3) into Eq. (4) yields

$$\begin{aligned} |R(\lambda)|^2 = & 1 + \frac{1}{576} k^8 |\lambda|^8 - \frac{1}{72} k^6 |\lambda|^6 + \left(\frac{k^6 |\lambda|^6}{6} - k^4 |\lambda|^4 + 24 \right) \frac{k}{12} \text{Re}(\lambda) \\ & + (k^4 |\lambda|^4 + 24) \frac{k^2}{12} (\text{Re}(\lambda))^2 + (k^2 |\lambda|^2 + 4) \frac{k^3}{3} (\text{Re}(\lambda))^3 + \frac{2k^4}{3} (\text{Re}(\lambda))^4. \end{aligned} \quad (5)$$

The stability of the RK4 scheme is guaranteed if

$$\|\vec{R}(\vec{p})\|_{\infty} < 1, \quad (6)$$

where $\|\cdot\|_{\infty}$ denotes the infinity norm defined as $\|\vec{x}\|_{\infty} = \max\{|x_0|, |x_1|, \dots, |x_{N-1}|\}$. In Fig. 1 we show the stability region for the RK4 scheme given by Eq. (6) as well as that for lower-order Runge-Kutta schemes (which use progressively truncated versions of Eq. (4)) [5]. As we shall show, the eigenvalues of the \mathcal{A} matrix are all purely imaginary (or nearly so) in the case of the nonlinear (and linear) Schrödinger equation. Thus, it can be seen from Fig. 1 that the third-order Runge-Kutta is the lowest-order RK scheme that is

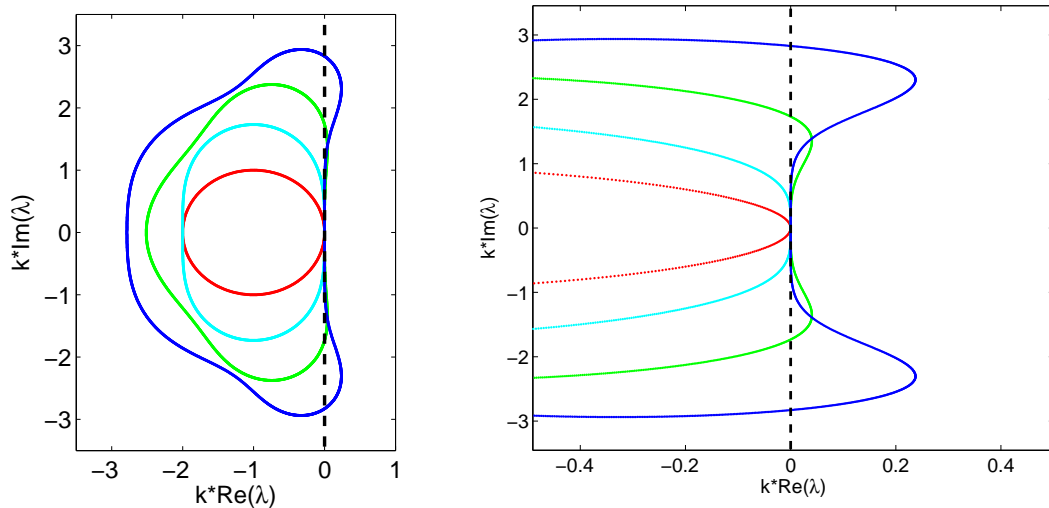


Figure 1: Left: Stability regions for Runge-Kutta schemes. Schemes from first-order to fourth-order are shown from center outwards. Right: Magnified view of the same plot near the point where $\text{Re}(\lambda) = 0$.

conditionally stable for the Schrödinger equations (however, as shown in Ref. [9], this is not the case if the real and imaginary parts of the NLSE are computed in a staggered time grid), while the RK4 yields a significantly larger bound on k . This is in contrast to similar PDEs such as the heat equation, whose \mathcal{A} matrix eigenvalues are typically all real-valued, in which case even forward differencing (RK1) is conditionally stable.

If $\text{Re}(\vec{\lambda}) = \vec{0}$, Eq. (5) simplifies greatly and becomes

$$|R(\vec{\lambda})|^2 = 1 + \frac{1}{576} k^8 |\vec{\lambda}|^8 - \frac{1}{72} k^6 |\vec{\lambda}|^6, \quad (7)$$

in which case, Eq. (6) leads to the simple stability bound

$$k < \frac{\sqrt{8}}{\|\vec{\lambda}\|_\infty}. \quad (8)$$

2.2 Application to the NLSE

Applying the stability theory of Sec. 2.1 to the NLSE has the obvious problem that the analysis is purely linear, while the NLSE has one (or more) nonlinear terms. A full nonlinear stability analysis is beyond the scope of this paper, so instead we linearize the problem by treating the nonlinearity ($|\Psi|^2$) as a constant value U (the external potential term is usually a constant, and so does not need any special treatment). This has been done previously for the one-dimensional coupled NLSE for fourth-order differencing (in the exclusive case where $s < 0$) in Ref. [8]. Since the value of $|\Psi|^2$ changes over time during the simulation, the linearized stability bound will also change over time. This change in many cases is expected to be small and therefore can be ignored, i.e. one may compute the bound using the initial condition of Ψ (and $V(\mathbf{r})$) and just leave a few percent leeway to cover any changes. This is especially true in the repulsive case ($s < 0$) where most situations have a constant-density background (or maximum background) and the dynamics do not cause the background value to change significantly (for example, when simulated coherent structures, most of the dynamics are translations of the initial condition with little change in structure). In attractive cases ($s > 0$), blow-up can occur which can alter the stability bound greatly, causing the simulation to crash (although in such a case the wavefunction is exploding towards infinity, which most finite-difference schemes cannot

handle anyways). Many times, simulations of a steady-state or near-steady-state in the modulus-squared with a constant potential are performed. In such situations, the linearized stability bounds will be (nearly) exact.

It is useful to also formulate stability bounds for the basic linear Schrödinger equation (where $s = 0$ and $V(\mathbf{r}) = 0$). In addition to providing bounds for the LSE, the results can also be used as practical estimates of the stability bounds for the NLSE (the discrepancy can often be solved by lowering the bound by a few percent).

2.3 Stability Analysis Procedure

In order to simplify the analysis, we first rewrite Eq. (2) as

$$\frac{\partial \vec{\Psi}}{\partial t} = \mathcal{A} \vec{\Psi} = \frac{i a}{h^2} A \vec{\Psi},$$

where h is the step size of the spatial finite-difference scheme being used. Then, assuming all eigenvalues of A are real-valued, the stability condition of Eq. (8) becomes

$$k < \frac{\sqrt{8}}{\|\vec{\lambda}_A\|_\infty} \frac{h^2}{a}. \quad (9)$$

In order to be able to use the stability bound of Eq. (9), we must first confirm that all eigenvalues of A are purely real (or nearly so) for each scheme/boundary condition combination. In cases where the eigenvalues are not able to be easily computed analytically, we show that the A matrix's eigenvalues are a set of boundary values with the remaining eigenvalues being those of a symmetric matrix denoted A' . Then by Theorem 1, it is known that all the eigenvalues of A are real.

Theorem 1 (Ref. [10]). *The eigenvalues of a real symmetric matrix are real.*

Once it has been established that Eq. (9) can be used, in order to get an upper-bound on k , we require an upper-bound on the maximum absolute eigenvalue of A . Due to the sparsity and diagonal dominance of A , a good estimate of the upper-bound can be found using the Gershgorin circle theorem (Definition 1 and Theorem 2).

Definition 1 (Ref. [11]). *Let A be a square complex matrix. Around every element a_{ii} on the diagonal of the matrix, a circle with radius equal to the sum of the norms of the other elements in the same row ($\sum_{j \neq i} |a_{ij}|$) is known as a Gershgorin disc.*

Theorem 2 (Ref. [11]). *Every eigenvalue of a square complex matrix A lies in one of its Gershgorin discs.*

Since every eigenvalue must be contained in a Gershgorin disk, by finding the maximum absolute value of the limits of the disks will yield an upper-bound on the maximum modulus of the eigenvalues of A .

In the one-dimensional LSE case with no external potential and periodic boundary conditions, the A matrix becomes circulant as defined by Definition 2. In this case, the eigenvalues can be computed analytically by Theorem 3. The upper-bound is then taken by finding the limit of the maximum eigenvalue as the size of the matrix goes to infinity.

Definition 2 (Ref. [11]). *A circulant matrix is a square $N \times N$ matrix C that can be fully specified by one vector, $\vec{c} = \{c_0, c_1, \dots, c_{N-1}\}$, which appears as the first column of C . The remaining columns of C are each cyclic permutations of the vector with the offset equal to the column index.*

Theorem 3 (Ref. [11]). *The eigenvalues of a circulant matrix are given by*

$$\lambda_j = c_0 + c_{N-1} \omega_j + c_{N-2} \omega_j^2 + \dots + c_1 \omega_j^{N-1}, \quad j = 0, \dots, N-1,$$

where

$$\omega_j = \exp\left(\frac{2\pi i j}{N}\right).$$

3 Boundary Conditions

Since boundary conditions can alter the stability of a scheme dramatically, it is necessary to have stability results for each specific boundary condition one would like to use. In this paper we limit ourselves to four boundary conditions which we feel are the best combination of simplicity and usefulness. These boundary conditions are: periodic, Dirichlet, Laplacian-zero, and Modulus-Squared-Dirichlet. As notation, we use the subscript b to represent any boundary point, and $b - 1$ to represent the grid position one point inward from the boundary in the normal direction.

For use with the stability analysis, it is desirable to formulate each boundary condition in terms of the temporal derivative in the form

$$\left. \frac{\partial \Psi}{\partial t} \right|_b = \frac{i a}{h^2} B_b \Psi_b, \quad (10)$$

and in terms of the spatial Laplacian in the form

$$\nabla^2 \Psi_b = \frac{1}{h^2} D_b \Psi_b, \quad (11)$$

where B_b and D_b are assumed to be real-valued constants (possibly differing per boundary point) and defined based on the specific boundary condition being used. For periodic boundary conditions (or linear one-sided conditions not discussed here), these forms are not applicable. Writing the boundary conditions in the forms of Eq. (10) and Eq. (11) allows the boundary conditions to be expressed in the A matrix as a single real-valued entry (B_b), and in the case of the fourth-order differencing, the near-boundary interior points will simply contain D_b in their formulation.

3.1 Periodic

For periodic boundary conditions, any element of the scheme that is too small or too large in index (i.e. they are 'off the grid') are simply replaced by the grid points on the opposite side of the grid. In the case of the NLSE, periodic boundary conditions can be problematic especially in background-density situations due to the unpredictable phase jump from one side of the grid to the other.

3.2 Dirichlet

Dirichlet boundary conditions are defined as

$$\Psi_b = c$$

where c is a constant, often zero. A more useful expression of this condition for use with the RK4 is

$$\left. \frac{\partial \Psi}{\partial t} \right|_b = 0,$$

in which case $B_b = 0$. When inserted into the NLSE, the condition in terms of the Laplacian is given by

$$\nabla^2 \Psi_b = -\frac{1}{a} (s |\Psi_b|^2 - V_b) \Psi_b,$$

and therefore $D_b = -\frac{h^2}{a} (s |\Psi_b|^2 - V_b)$.

3.3 Modulus-Squared Dirichlet

In some situations Dirichlet boundary condition can fail. failure typically occurs in simulations with a constant-density background, i.e. a constant value of $|\Psi|^2$ at the boundaries. A standard Dirichlet condition will not work in this case because it does not handle the phase rotation (remember that Ψ is a complex field).

Instead, one would like to have the modulus-squared of the wavefunction to be constant at the boundaries, i.e.

$$|\Psi_b|^2 = c,$$

where c is a constant. We have recently formulated a method for such a boundary condition (which is almost as easy to implement as Dirichlet) called the modulus-squared Dirichlet (MSD) boundary condition [7]. The MSD boundary condition is defined as,

$$\frac{\partial \Psi}{\partial t} \Big|_b \approx \frac{\partial \Psi}{\partial t} \Big|_{b-1} \frac{\Psi_b}{\Psi_{b-1}}, \quad (12)$$

where $\frac{\partial \Psi}{\partial t} \Big|_{b-1}$ is computed by the interior scheme first, and then used to compute the boundary values. Using the MSD boundary condition gives $B_b = \frac{\hbar^2}{i a} \frac{\partial \Psi}{\partial t} \Big|_{b-1} \frac{1}{\Psi_{b-1}}$, which is nonlinear, not a constant, and at first glance does not seem to be real-valued. However, as shown in Ref. [7], due to the underlying assumptions of the MSD boundary condition, Eq. (12) can be viewed as

$$\frac{\partial \Psi}{\partial t} \Big|_b \approx i \Omega_{b-1} \Psi_b,$$

where Ω_{b-1} is the real-valued frequency of the solution near the boundary. Thus, B_b would have the form $B_b = \frac{\hbar^2}{a} \Omega_{b-1}$, which is real-valued. Therefore, we can linearize the MSD boundary condition by treating the B_b term as a constant (which can change over the course of the simulation, similar to the nonlinearity of the NLSE). The small imaginary part of B_b that may appear in the simulation is negligible, and therefore B_b will not add any significant imaginary part to the eigenvalues of A .

When inserted into the NLSE, the MSD boundary condition of Eq. (12) yields

$$\nabla^2 \Psi_b \approx \left[\frac{\nabla^2 \Psi_{b-1}}{\Psi_{b-1}} + \frac{1}{a} (V_b - V_{b-1} + s[|\Psi_{b-1}|^2 - |\Psi_b|^2]) \right] \Psi_b, \quad (13)$$

and therefore $D_b = \hbar^2 \left[\frac{\nabla^2 \Psi_{b-1}}{\Psi_{b-1}} + \frac{1}{a} (V_b - V_{b-1} + s[|\Psi_{b-1}|^2 - |\Psi_b|^2]) \right]$. This too is a nonlinear non-constant term that may contain an imaginary part. However, as we will show in Secs. 4.2.2, 5.2, and 6.2, the D_b terms do not enter into the bounds of the eigenvalues, and therefore do not cause the eigenvalues to become imaginary.

3.4 Laplacian-Zero Boundary Condition

The Laplacian-zero boundary condition is a simplified ad-hoc version of a no-flux condition which is given by

$$\nabla^2 \Psi_b = 0,$$

and therefore $D_b = 0$. The NLSE-specific RK4-friendly version is

$$\frac{\partial \Psi}{\partial t} \Big|_b = i (s |\Psi_b|^2 - V_b) \Psi_b,$$

making $B_b = \frac{\hbar^2}{a} (s |\Psi_b|^2 - V_b)$. This condition is as easy to implement as the Dirichlet, and can be useful in many situations.

We summarize the values of B_b and D_b for the various boundary conditions in Table. 1. Many other boundary conditions exist for simulating the NLSE, but ideally, the analysis shown here can be adapted to the chosen boundary conditions.

Table 1: Boundary condition terms for use with stability analysis.

Boundary Condition	B_b	D_b
Dirichlet	0	$\frac{h^2}{a}(V_b - s \Psi_b ^2)$
Laplacian-zero	$\frac{h^2}{a}(s \Psi_b ^2 - V_b)$	0
MSD	$\frac{h^2}{i a} \frac{1}{\Psi_{b-1}} \frac{\partial \Psi}{\partial t} \Big _{b-1}$	$h^2 \left[\frac{\nabla^2 \Psi_{b-1}}{\Psi_{b-1}} + \frac{1}{a}(V_b - V_{b-1} + s[\Psi_{b-1} ^2 - \Psi_b ^2]) \right]$

4 One-Dimensional Stability Analysis

In the one-dimensional cases we analyze all four boundary conditions mentioned in Sec. 3. As stated, periodic boundary conditions yield a matrix where (in the linear case with $s = 0$ and $\vec{V}(\mathbf{r}) = 0$) the eigenvalues can be computed analytically. This allows the comparison of our upper-bound methods (which we use with other boundary conditions) with the true eigenvalues. This will give a good idea as to how close to the true upper-bound these methods are.

4.1 Second-Order Central Difference

The second-order central difference is considered to be the standard finite-difference scheme for the second spatial derivative. It is given by

$$\nabla^2 \Psi_i = \frac{\partial^2 \Psi}{\partial x^2} \Big|_i \approx \frac{\Psi_{i+1} - 2\Psi_i + \Psi_{i-1}}{h^2},$$

and when implemented into the A matrix, forms a matrix which is tridiagonal (except for the boundary condition rows).

4.1.1 Periodic Boundary Conditions

In order to obtain analytic expressions for the eigenvalues of A , we start with the LSE case with no external potential and periodic boundary conditions. This yields the matrix

$$A = \begin{bmatrix} -2 & 1 & 0 & 0 & 1 \\ 1 & -2 & 1 & 0 & 0 \\ 0 & \ddots & \ddots & \ddots & 0 \\ 0 & 0 & 1 & -2 & 1 \\ 1 & 0 & 0 & 1 & -2 \end{bmatrix},$$

which is a circulant matrix with $\vec{c} = \{-2, 1, 0, \dots, 0, 1\}$. Also, since A is a real-valued symmetric matrix, by Theorem 1, all eigenvalues are real and therefore the stability criteria of Eq. (9) can be used. By Theorem 3, the eigenvalues of A are given by

$$\lambda_j = -2 + \exp \left[\frac{2\pi i j}{N} \right] + \exp \left[\frac{2\pi i j(N-1)}{N} \right], \quad j \in \{0, \dots, N-1\}.$$

The maximum value of $|\lambda_j|$ occurs either at $j = N/2$ if N is even, or $j = (N \pm 1)/2$ if N is odd. For N even-valued we have

$$|\lambda|_{\max} = \left| -2 + \exp[\pi i] + \exp[\pi i]^{N-1} \right|,$$

which yields

$$|\lambda|_{\max} = 4.$$

For N odd-valued we have

$$|\lambda|_{\max} = \left| -2 - (-1)^{1/N} + (-1)^N (-1)^{-1/N} \right|,$$

which yields

$$|\lambda|_{\max} = \left| -2 - 2 \cos\left(\frac{\pi}{N}\right) \right|.$$

Taking $N \rightarrow \infty$, the maximum bound on the maximum absolute eigenvalue becomes

$$|\lambda|_{\max} < 4.$$

We therefore have an upper bound on the maximum absolute eigenvalue which, for even-valued N , is guaranteed to be one of the eigenvalues. The stability criteria is then formulated as

$$k < \frac{\sqrt{8} h^2}{4 a}. \quad (14)$$

In the general case where $s \neq 0$ and/or $V(\mathbf{r}) \neq 0$, the A matrix is no longer circulant (since the values of the nonlinearity or external potential vary over the diagonal of A). To get a bound on the maximum absolute eigenvalue, we make use of Theorem 2. There are N Gershgorin disks, since each diagonal entry of A can be unique, but each disk has the same radius 1. Also, since the diagonal entries can in theory take on any value, both Gershgorin disk limits must be examined. This yields the stability bound

$$k < \frac{\sqrt{8}}{\max\{\|\vec{L}\|_{\infty}, \|\vec{L} - 4\|_{\infty}\}} \frac{h^2}{a}, \quad (15)$$

where we have defined the elements of \vec{L} to be

$$L_i = \frac{h^2}{a} (s |\Psi_i|^2 - V_i), \quad (16)$$

where the index i spans over the entire grid. It is important to note that all values of \vec{L} in the denominator of the stability bound are $O(h^2)$. Thus, for $h \ll 1$, and reasonable values of \vec{L} , the linear bound of Eq. (14) should be very close to the true bound of the nonlinear problem.

If we set $\vec{L} = 0$ in Eq. (15), we recover the bound in Eq. (14). This shows that (in this case at least), using the Gershgorin circle theorem yields the true bound on the eigenvalues of A .

4.1.2 Dirichlet, Laplacian-zero, and Modulus-Squared Dirichlet Boundary Conditions

As shown in Sec. 3, Dirichlet, Laplacian-zero, and modulus-squared Dirichlet boundary conditions can all be viewed as single entries in the boundary value rows of the A matrix, denoted as B_b . As shown there, the values of B_b are assumed to be real-valued and their values for each BC were given in Table 1. Using such a formulation, the A matrix becomes

$$A = \begin{bmatrix} B_0 & 0 & 0 & 0 & 0 \\ 1 & L_1 - 2 & 1 & 0 & 0 \\ 0 & \ddots & \ddots & \ddots & 0 \\ 0 & 0 & 1 & L_{N-2} - 2 & 1 \\ 0 & 0 & 0 & 0 & B_{N-1} \end{bmatrix}.$$

In order to use the simple stability criteria of Eq. (9), we once again need to show that all eigenvalues of A are purely real. The A matrix is no longer symmetric, however it is easy to see that B_0 and B_{N-1} are eigenvalues of A , and the remaining eigenvalues of A are equivalent to the eigenvalues of the matrix A' defined as

$$A' = \begin{bmatrix} L_1 - 2 & 1 & 0 & 0 & 0 \\ 1 & L_2 - 2 & 1 & 0 & 0 \\ 0 & \ddots & \ddots & \ddots & 0 \\ 0 & 0 & 1 & L_{N-2} - 2 & 1 \\ 0 & 0 & 0 & 1 & L_{N-1} - 2 \end{bmatrix}.$$

Since A' is real-valued symmetric, we can use the stability bound of Eq. (9).

We now need to find an upper bound on the absolute value of the eigenvalues of A' . We use the Gershgorin circle theorem to find all unique Gershgorin disks and take the limits of the disks to find the bounds on the absolute eigenvalues. Many of the Gershgorin disks are similar, differing only in the value of L_i of the specific row. Therefore, each disk form has a subset of L_i values relevant to it. Although in the current one-dimensional setting it is simple to define the subsets, in higher-dimensional settings, it can become burdensome to separate out each subset of \vec{L} relevant to each Gershgorin disk form. Therefore, for practicality purposes, we define our bounds using all possible values of L_i for each Gershgorin disk. This may make the resulting stability bound slightly higher than necessary in certain cases, but this is outweighed by the ease-of-use of the simplified bounds.

Table 2: Unique forms of the Gershgorin disk centers and radii for the A' matrix of the one-dimensional second-order central difference scheme.

a_{ii}	$r_i = \sum_{i \neq j} a_{ij} $
$L_i - 2$	1
$L_i - 2$	2

The unique forms of the Gershgorin disks of A' are shown in Table 2. The resulting general stability bounds are

$$k < \frac{\sqrt{8}}{\max\{\|\vec{B}\|_\infty, \|\forall L_i, L_i - \vec{G}\|_\infty\}} \frac{h^2}{a}, \quad (17)$$

where \vec{B} are all boundary condition values (in this case B_0 and B_{N-1}), and \vec{G} is defined as

$$\vec{G} = \{4, 3, 1, 0\}. \quad (18)$$

In general, all possible values of \vec{G} must be taken into consideration since there is no theoretical restriction on what values \vec{L} can take. However, in certain specific circumstances, some of the values of \vec{G} can be ignored (for example, when $s \leq 0$ and $V(\mathbf{r}) \geq 0$ only the largest magnitude value in \vec{G} is needed).

4.2 Fourth Order Central Difference

The standard fourth order central difference scheme is given by

$$\nabla^2 \Psi_i = \frac{\partial^2 \Psi}{\partial x^2} \Big|_i \approx \frac{-\Psi_{i+2} + 16\Psi_{i+1} - 30\Psi_i + 16\Psi_{i-1} - \Psi_{i-2}}{12h^2}. \quad (19)$$

The stability analysis follows directly from the second-order case. The only major difference is that since the fourth order stencil is five points wide, the grid points near the boundary may need special consideration for

the different boundary conditions. For our purposes here, we use the two-step high-order compact (2SHOC) version of the fourth-order scheme as described in Ref. [6], in which case the near-boundary points are formulated based on the boundary condition of the Laplacian.

4.2.1 Periodic Boundary Condition

In the periodic case, no special attention is needed near the boundaries, and the A matrix in the LSE case with no external potential is

$$A = \begin{bmatrix} -15/6 & 4/3 & -1/12 & 0 & 0 & -1/12 & 4/3 \\ 4/3 & -15/6 & 4/3 & -1/12 & 0 & 0 & -1/12 \\ -1/12 & 4/3 & -15/6 & 4/3 & -1/12 & 0 & 0 \\ 0 & \ddots & \ddots & \ddots & \ddots & \ddots & 0 \\ 0 & 0 & -1/12 & 4/3 & -15/6 & 4/3 & -1/12 \\ -1/12 & 0 & 0 & -1/12 & 4/3 & -15/6 & 4/3 \\ 4/3 & -1/12 & 0 & 0 & -1/12 & 4/3 & -15/6 \end{bmatrix},$$

which is a circulant matrix, and its eigenvalues are given by

$$\lambda_j = -\frac{15}{6} + \frac{4}{3} \exp\left[\frac{2\pi ij}{N}\right] - \frac{1}{12} \exp\left[\frac{4\pi ij}{N}\right] - \frac{1}{12} \exp\left[\frac{2(N-2)\pi ij}{N}\right] + \frac{4}{3} \exp\left[\frac{2(N-1)\pi ij}{N}\right].$$

The maximum absolute value once again occurs at either $j = N/2$ if N is even, or $j = (N \pm 1)/2$ if N is odd. For N even-valued we have

$$\lambda_{N/2} = -\frac{15}{6} - \frac{4}{3} - \frac{1}{12} - \frac{1}{12}(-1)^{N-2} + \frac{4}{3}(-1)^{N-1} = -\frac{16}{3}.$$

For N odd, we have

$$\lambda_{(N+1)/s} = -\frac{15}{6} - \frac{4}{3} \left((-1)^{1/N} + (-1)^{-1/N} \right) - \frac{1}{12} \left((-1)^{2/N} + (-1)^{-2/N} \right),$$

which yields

$$\lambda_{(N+1)/s} = -\frac{15}{6} - \frac{4}{3} \left(2 \cos\left(\frac{\pi}{N}\right) \right) - \frac{1}{12} \left(2 \cos\left(\frac{2\pi}{N}\right) \right).$$

As $N \rightarrow \infty$, $|\lambda| \rightarrow \frac{16}{3}$, which is the same bound as the N -even case. thus, the stability bound is given by

$$k < \left(\frac{3}{4}\right) \frac{\sqrt{8} h^2}{4 a},$$

which is only 75% of the second-order bound of Eq. (14). In the general case where $\vec{L} \neq 0$, we get the bound

$$k < \frac{6\sqrt{2}}{\max\{\|3\vec{L} - 16\|_\infty, \|3\vec{L} + 1\|_\infty\}} \frac{h^2}{a}.$$

If $s \leq 0$ and $V(\mathbf{r}) \geq 0$, the first term in the denominator is the maximum of the two terms, and the resulting stability bound is equivalent to that found for the coupled NLSE in Ref. [8].

4.2.2 Dirichlet, Modulus-Squared Dirichlet, and Laplacian-zero Boundary Conditions

As per Sec. 3, we formulate all three boundary conditions in terms of a B_b entry in the A matrix. As discussed, an important issue is that we need to handle the grid points near the boundary due to the width of the scheme. One way of dealing with the closest-interior points is to compute the Laplacian at those points using the second-order differencing, however this can lead to the overall scheme becoming second order. Instead, we use the 2SHOC formulation of the fourth-order differencing which allows us to derive the closest-interior points which, if the assumptions of the chosen boundary conditions hold, should maintain fourth order accuracy. In one dimension, the 2SHOC scheme is defined as [6]

$$1) \quad D_i = \frac{1}{h^2} (\Psi_{i+1} - 2\Psi_i + \Psi_{i-1}), \quad (20)$$

$$2) \quad \nabla^2 \Psi_i \approx \frac{7}{6} D_i - \frac{1}{12} (D_{i+1} + D_{i-1}). \quad (21)$$

In the first step, the second-order Laplacian is computed with the chosen boundary condition applied to it. Next, the result is used to compute the fourth-order Laplacian. Algebraically, this two-step scheme is equivalent to the standard wide-stencil of Eq. (19). We use the form of Eq. (11) for the boundary conditions on the Laplacian, and after combining the steps of Eq. (20) and Eq. (21), we get the matrix

$$A = \begin{bmatrix} B_0 & 0 & 0 & 0 & 0 & 0 & 0 \\ \frac{14-D_0}{12} & L_1 - 29/12 & 4/3 & -1/12 & 0 & 0 & 0 \\ -1/12 & 4/3 & L_2 - 15/6 & 4/3 & -1/12 & 0 & 0 \\ 0 & \ddots & \ddots & \ddots & \ddots & \ddots & 0 \\ 0 & 0 & -1/12 & 4/3 & L_{N-3} - 15/6 & 4/3 & -1/12 \\ 0 & 0 & 0 & -1/12 & 4/3 & L_{N-2} - 29/12 & \frac{14-D_{N-1}}{12} \\ 0 & 0 & 0 & 0 & 0 & 0 & B_{N-1} \end{bmatrix}$$

The B_b and D_b terms for each boundary condition are once again given in Table 1. As in Sec. 4.1.2, the A matrix is not symmetric and has eigenvalues equal to \vec{B} . The remaining eigenvalues are those of the matrix A' defined as

$$A' = \begin{bmatrix} L_1 - 29/12 & 4/3 & -1/12 & 0 & 0 & 0 & 0 \\ 4/3 & L_2 - 15/6 & 4/3 & -1/12 & 0 & 0 & 0 \\ -1/12 & 4/3 & L_3 - 15/6 & 4/3 & -1/12 & 0 & 0 \\ 0 & \ddots & \ddots & \ddots & \ddots & \ddots & 0 \\ 0 & 0 & -1/12 & 4/3 & L_{N-4} - 15/6 & 4/3 & -1/12 \\ 0 & 0 & 0 & -1/12 & 4/3 & L_{N-3} - 15/6 & 4/3 \\ 0 & 0 & 0 & 0 & -1/12 & 4/3 & L_{N-2} - 29/12 \end{bmatrix}.$$

A' is once again real-symmetric so the bounds of Eq. (9) can be used. It is interesting to note that the values of D_b do not appear in any of the eigenvalues of A' .

The unique forms (see the discussion in Sec. 4.1.2) of the Gershgorin disk centers and radii are shown in Table 3. The full stability bound is the same as Eq. (17), but with \vec{G} defined as

$$\vec{G} = \frac{1}{12} \times \{64, 63, 46, 12, -3, -4\}. \quad (22)$$

Table 3: Unique forms of the Gershgorin disk centers and radii for the A' matrix of the one-dimensional fourth-order 2SHOC scheme.

a_{ii}	$r_i = \sum_{i \neq j} a_{ij} $
$L_i - 5/2$	$11/4$
$L_i - 5/2$	$17/6$
$L_i - 29/12$	$17/12$

5 Two-Dimensional Stability Analysis

In higher dimensions, the A matrix is formed by unwrapping the solution into a one-dimensional vector and then formulating the scheme matrix accordingly.

In Sections 4.1.1 and 4.2.1 we noted that the stability bounds given using the Gershgorin circle theorem were equivalent to those obtained analytically for the linear case with periodic boundary conditions. We therefore justify relying exclusively on the Gershgorin theorem for higher dimensions, and focus on the stability bounds for Dirichlet, MSD, and Laplacian-zero boundary conditions (since the periodic boundary condition bounds will be a subset of the bounds computed for the other boundary conditions).

5.1 Second-Order Central Differencing

The second-order central difference scheme in two dimensions is given by

$$\nabla^2 \Psi_{i,j} = \frac{\partial^2 \Psi}{\partial x^2} \Big|_{i,j} + \frac{\partial^2 \Psi}{\partial y^2} \Big|_{i,j} \approx \frac{1}{h^2} \begin{bmatrix} & & 1 & & \\ & 1 & -4 & 1 & \\ & & 1 & & \end{bmatrix} \Psi_{i,j}. \quad (23)$$

The corresponding A matrix has a tri-banded structure, with diagonal sub-sections corresponding to the boundary values. The form of the A matrix is shown in Fig. 2 (we do not show the values of the entries of the matrix for space considerations, they can be obtained through symbolic codes available upon request). As in the one-dimensional case, all diagonal entries (which are the boundary value entries B_b) of A are eigenvalues, and the remaining eigenvalues are real and equivalent to those of a matrix A' which is real-symmetric, thus allowing the use of the bounds in Eq. (9). The form of A' is also shown in Fig. 2.

The unique forms of the Gershgorin disk centers and radii for A' are shown in Table 4. The stability bounds are the same as in Eq. (17) with \vec{B} being the set of all boundary values B_b and with \vec{G} now defined as

$$\vec{G} = \{0, 1, 2, 6, 7, 8\}. \quad (24)$$

In the linear case ($s = 0$) with no external potential and periodic, Dirichlet or Laplacian-zero boundary conditions, we get the linear stability bound

$$k < \frac{\sqrt{8}}{8} \frac{h^2}{a}. \quad (25)$$

Table 4: Gershgorin disk centers and radii for the A' matrix of the two-dimensional central difference scheme.

a_{ii}	$r_i = \sum_{i \neq j} a_{ij} $
$L_i - 4$	2
$L_i - 4$	3
$L_i - 4$	4

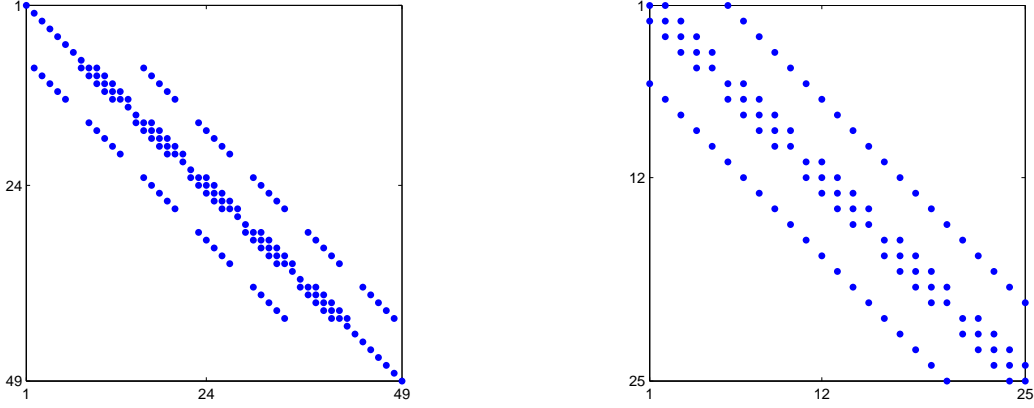


Figure 2: Form of scheme matrix A and A' for second-order central differencing of the two-dimensional NLSE. The dots represent non-zero entries of the matrices. The matrices shown are for a 7×7 grid.

As before, since within the A matrix, all boundary, potential, and nonlinear terms are $O(h^2)$ the simple bound of Eq. (25) with slight adjustment can be used in practical applications.

5.2 Fourth-Order Central Differencing

The fourth-order central difference scheme in two dimensions is given by

$$\nabla^2 \Psi_{i,j} \approx -\frac{1}{12h^2} \begin{array}{ccccc} & & 1 & & \\ & & -16 & & \\ 1 & -16 & 60 & -16 & 1 \\ & & -16 & & \\ & & 1 & & \end{array} \Psi_{i,j}. \quad (26)$$

The low-storage version of the 2SHOC equivalent scheme is defined as [6]

$$1) \quad D_{i,j} = \frac{1}{h^2} \begin{array}{ccc} & 1 & \\ 1 & -4 & 1 \\ & 1 & \end{array} \Psi_{i,j} \quad (27)$$

$$2) \quad \nabla^2 \Psi_{i,j} \approx -\frac{1}{12} \begin{array}{ccc} & 1 & \\ 1 & -12 & 1 \\ & 1 & \end{array} D_{i,j} + \frac{1}{6h^2} \begin{array}{ccc} 1 & & 1 \\ & -4 & \\ 1 & & 1 \end{array} \Psi_{i,j}. \quad (28)$$

and the corresponding A matrix has a five-banded structure. The structure of the A matrix and its corresponding A' matrix (see Sec. 5.1) are shown in Fig. 3.

The unique forms of the Gershgorin disk centers and radii for A' are shown in Table 5. The stability bound is then the same as Eq. (17) with \vec{G} defined as

$$\vec{G} = \frac{1}{12} \times \{128, 127, 126, 110, 109, 92, 24, 9, 8, -6, -7, -8\}. \quad (29)$$

The linear bound ($s = 0$ and $V(\mathbf{r}) = 0$) is then given by

$$k < \frac{3\sqrt{8}}{32} \frac{h^2}{a}, \quad (30)$$

which, as in the one-dimensional case, is simply $3/4$ of the second-order bound given in Eq. (25).

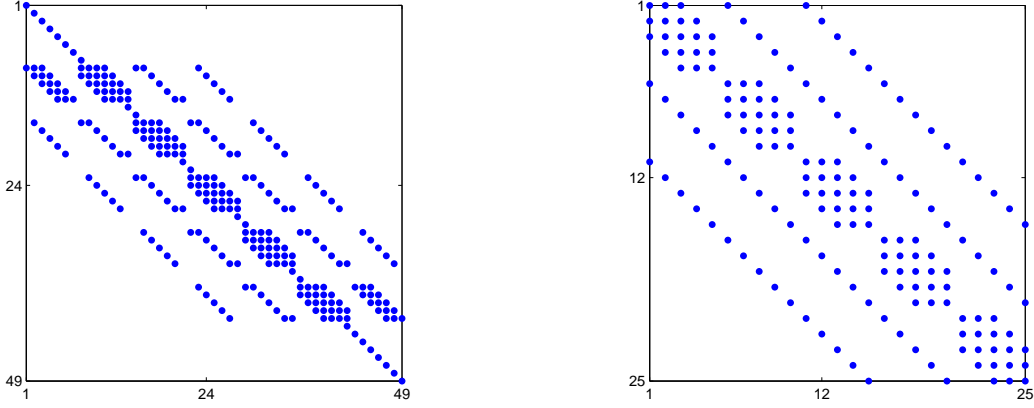


Figure 3: Form of scheme matrix A and A' for the fourth-order 2SHOC scheme of the two-dimensional NLSE. The dots represent non-zero entries of the matrices. The matrices shown are for a 7×7 grid.

Table 5: Gershgorin disk centers and radii for the A' matrix of the two-dimensional 2SHOC scheme.

a_{ii}	$r_i = \sum_{i \neq j} a_{ij} $
$L_i - 5$	$11/2$
$L_i - 5$	$67/12$
$L_i - 5$	$17/3$
$L_i - 29/6$	$17/6$
$L_i - 59/12$	$25/6$
$L_i - 59/12$	$17/4$

6 Three-Dimensional Stability Analysis

For the stability analysis in three dimensions, the same procedure as in the two-dimensional case of Sec. 5 will be used.

6.1 Second-Order Central Differencing

The second-order central difference scheme in three dimensions is given by

$$\begin{aligned}
 \nabla^2 \Psi_{i,j,k} &= \frac{\partial^2 \Psi}{\partial x^2} \Big|_{i,j,k} + \frac{\partial^2 \Psi}{\partial y^2} \Big|_{i,j,k} + \frac{\partial^2 \Psi}{\partial z^2} \Big|_{i,j,k} \\
 &\approx \frac{1}{h^2} \left(\begin{array}{|c|c|c|} \hline & & \\ \hline & 1 & \\ \hline & & \\ \hline \end{array} \Psi_{i,j+1,k} + \begin{array}{|c|c|c|} \hline & 1 & \\ \hline 1 & -6 & 1 \\ \hline & 1 & \\ \hline \end{array} \Psi_{i,j,k} + \begin{array}{|c|c|c|} \hline & & \\ \hline & 1 & \\ \hline & & \\ \hline \end{array} \Psi_{i,j-1,k} \right), \tag{31}
 \end{aligned}$$

and the structure of the corresponding A and A' matrix are given in Fig. 4.

The unique forms of the Gershgorin disk centers and radii for A' are shown in Table 6. The stability bounds are the same as in Eq. (17), but with \vec{G} now defined as

$$\vec{G} = \{12, 11, 10, 9, 3, 2, 1, 0\}. \tag{32}$$

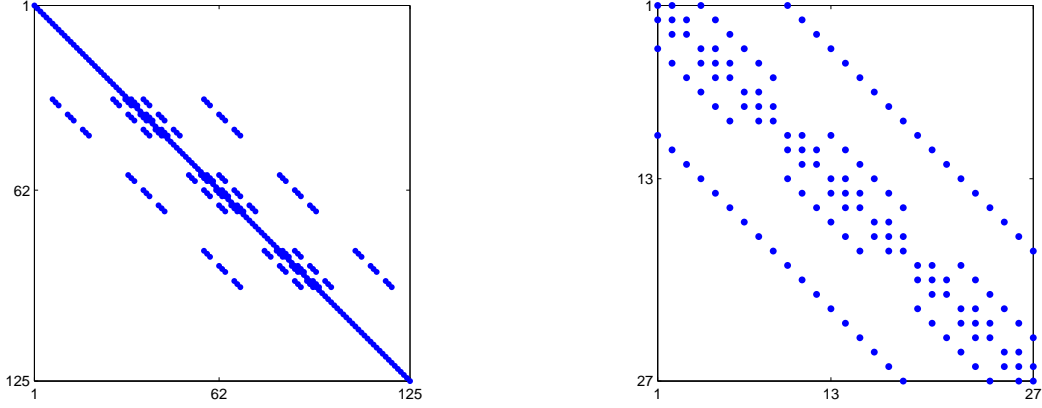


Figure 4: Form of scheme matrix A and A' for the second-order central difference scheme of the three-dimensional NLSE. The dots represent non-zero entries of the matrices. The matrices shown are for a 5×5 grid.

Table 6: Gershgorin disk centers and radii for the A' matrix of the three-dimensional central difference scheme.

a_{ii}	$r_i = \sum_{i \neq j} a_{ij} $
$L_i - 6$	3
$L_i - 6$	4
$L_i - 6$	5
$L_i - 6$	6

In the linear case ($s = 0$) with no external potential and periodic, Dirichlet or Laplacian-zero boundary conditions, we get the linear stability bound

$$k < \frac{\sqrt{8}}{12} \frac{h^2}{a}. \quad (33)$$

6.2 Fourth-Order Differencing

The fourth-order central difference scheme in three dimensions is given by

$$\begin{aligned} \nabla^2 \Psi \approx & \frac{1}{12h^2} [\Psi_{i+2,j,k} + \Psi_{i-2,j,k} + \Psi_{i,j+2,k} + \Psi_{i,j-2,k} + \Psi_{i,j,k+2} + \Psi_{i,j,k-2} \\ & - 16(\Psi_{i+1,j,k} + \Psi_{i-1,j,k} + \Psi_{i,j+1,k} + \Psi_{i,j-1,k} + \Psi_{i,j,k+1} + \Psi_{i,j,k-1}) + 90\Psi_{i,j,k}]. \end{aligned} \quad (34)$$

The single-storage version of the 2SHOC equivalent scheme is defined as [6]

$$1) \quad D_{i,j,k} = \frac{1}{h^2} \left(\begin{array}{|c|c|c|} \hline & & \\ \hline & 1 & \\ \hline & & \\ \hline \end{array} \Psi_{i,j+1,k} + \begin{array}{|c|c|c|} \hline & 1 & \\ \hline 1 & -6 & 1 \\ \hline & 1 & \\ \hline \end{array} \Psi_{i,j,k} + \begin{array}{|c|c|c|} \hline & & \\ \hline & 1 & \\ \hline & & \\ \hline \end{array} \Psi_{i,j-1,k} \right), \quad (35)$$

$$2) \quad \nabla^2 \Psi_{i,j,k} \approx -\frac{1}{12} \left(\begin{array}{|c|c|c|} \hline & & \\ \hline & 1 & \\ \hline & & \\ \hline \end{array} D_{i,j+1,k} + \begin{array}{|c|c|c|} \hline & 1 & \\ \hline 1 & -10 & 1 \\ \hline & 1 & \\ \hline \end{array} D_{i,j,k} + \begin{array}{|c|c|c|} \hline & & \\ \hline & 1 & \\ \hline & & \\ \hline \end{array} D_{i,j-1,k} \right) \quad (36)$$

$$+ \frac{1}{6h^2} \left(\begin{array}{|c|c|c|} \hline & 1 & \\ \hline 1 & & 1 \\ \hline & 1 & \\ \hline \end{array} \Psi_{i,j+1,k} + \begin{array}{|c|c|c|} \hline 1 & & 1 \\ \hline & -12 & \\ \hline 1 & & 1 \\ \hline \end{array} \Psi_{i,j,k} + \begin{array}{|c|c|c|} \hline & 1 & \\ \hline 1 & & 1 \\ \hline & 1 & \\ \hline \end{array} \Psi_{i,j-1,k} \right).$$

and the structure of the corresponding A and A' matrix are given in Fig. 5.

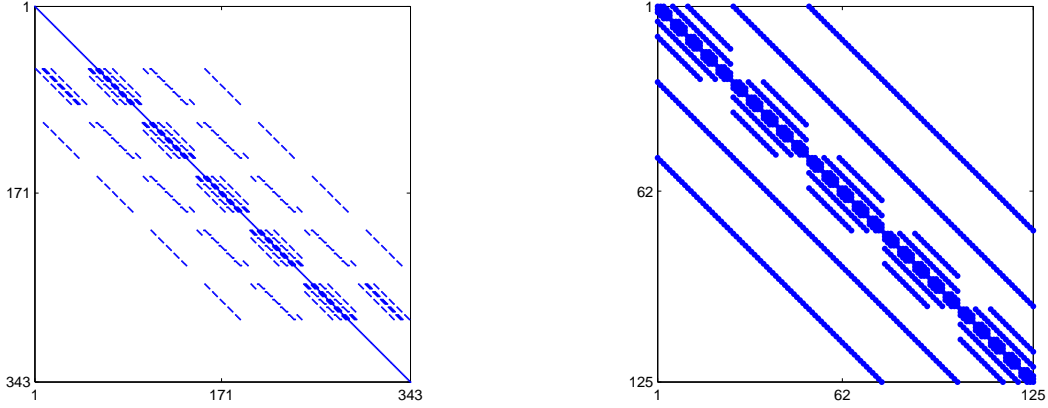


Figure 5: Form of scheme matrix A and A' for the fourth-order 2SHOC scheme of the three-dimensional NLSE. The dots represent non-zero entries of the matrices. The matrices shown are for a 7×7 grid.

Table 7: Gershgorin disk centers and radii for the A' matrix of the three-dimensional 2SHOC scheme.

a_{ii}	$r_i = \sum_{i \neq j} a_{ij} $
$L_i - 15/2$	$33/4$
$L_i - 15/2$	$25/3$
$L_i - 15/2$	$101/12$
$L_i - 15/2$	$17/2$
$L_i - 22/3$	$67/12$
$L_i - 22/3$	$17/3$
$L_i - 29/4$	$17/4$
$L_i - 89/12$	$83/12$
$L_i - 89/12$	7
$L_i - 89/12$	$85/12$

The unique forms of the Gershgorin disk centers and radii for A' are shown in Table 7. The stability

bounds are the same as in Eq. (17), but with \vec{G} now defined as

$$\vec{G} = \frac{1}{12} \times \{192, 191, 190, 189, 174, 173, 172, 156, 155, 138, 36, 21, 20, 6, 5, 4, -9, -10, -11, -12\}. \quad (37)$$

In the linear case ($s = 0$) with no external potential and periodic, Dirichlet or Laplacian-zero boundary conditions, we get the linear stability bound

$$k < \frac{\sqrt{8}}{16} \frac{h^2}{a}, \quad (38)$$

which, as in the one- and two-dimensional cases, is simply 3/4 of the second-order bound given in Eq. (33).

7 Conclusion and Summary of Results

In this paper we have formulated linearized stability bounds for using second- and fourth-order spacial finite-differencing with fourth-order Runge-Kutta time-stepping for the multi-dimensional nonlinear Schrödinger equation with Dirichlet, modulus-squared Dirichlet, Laplacian-zero, and periodic boundary conditions. For quick estimates, we provided linear results, while for a more accurate bound, the linearized results can be computed easily and implemented into simulation code, in order to use as large a time-step as possible which greatly increases efficiency in large-scale simulations.

We summarize the stability results as follows:

For the nonlinear Schrödinger equation (NLSE) defined as

$$i \frac{\partial \Psi}{\partial t} + a \nabla^2 \Psi - V(\mathbf{r}) \Psi + s |\Psi|^2 \Psi = 0,$$

where $a > 0$ and s are parameters of the system and $V(\mathbf{r})$ is an external potential, the numerical stability bounds on the time-step when using the fourth-order Runge-Kutta time-stepping scheme is as follows:

In the linear case where $s = 0$ and with no external potential ($V(\mathbf{r}) = 0$), utilizing periodic, Dirichlet, or Laplacian-zero boundary conditions, the stability bound on the time-step k when using the second-order central difference (CD) scheme in a d -dimensional setting is

$$k_{\text{CD}} < \frac{h^2}{d \sqrt{2} a}, \quad (39)$$

while that of using a fourth-order central difference scheme (with interior points computed in a two-step high-order compact (2SHOC) methodology [6]) is

$$k_{\text{2SHOC}} < \left(\frac{3}{4}\right) \frac{h^2}{d \sqrt{2} a}. \quad (40)$$

The linearized stability bounds for the general NLSE are

$$k < \frac{\sqrt{8}}{\max\{\|\vec{B}\|_\infty, \|\nabla L_i, L_i - \vec{G}\|_\infty\}} \frac{h^2}{a}, \quad (41)$$

where \vec{B} are the boundary points as defined by Table 8 (or in the periodic case is ignored), the elements of \vec{L} is defined as

$$L_i = \frac{h^2}{a} (s |\Psi_i|^2 - V_i),$$

where the index i spans the entire grid, and \vec{G} is a set of values defined in Table 9, determined by the dimension and method being used.

Table 8: Values for B_b for various boundary conditions.

	Dirichlet ($\Psi_b = \text{const}$)	Laplacian-zero ($\nabla^2 \Psi_b = 0$)	MSD ($ \Psi_b ^2 = \text{const}$)
B_b	0	$\frac{\hbar^2}{a} (s \Psi_b ^2 - V_b)$	$\frac{\hbar^2}{i a} \frac{1}{\Psi_{b-1}} \frac{\partial \Psi}{\partial t} \Big _{b-1}$

Table 9: Values for \vec{G} in Eq. (41).

Scheme	1D	2D	3D
CD $O(h^2)$	{4, 3, 1, 0}	{8, 7, 6, 2, 1, 0}	{12, 11, 10, 9, 3, 2, 1, 0}
2SHOC $O(h^4)$	$\frac{1}{12} \times \{64, 63, 46, 12, -3, -4\}$	$\frac{1}{12} \times \{128, 127, 126, 110, 109, 92, 24, 9, 8, -6, -7, -8\}$	$\frac{1}{12} \times \{192, 191, 190, 189, 174, 173, 172, 156, 155, 138, 36, 21, 20, 6, 5, 4, -9, -10, -11, -12\}$

Acknowledgments

This research was supported by NSF-DMS-0806762 and the Computational Science Research Center (CSRC) at SDSU. We gratefully acknowledge insightful discussions with Peter Blomgren.

References

- [1] L. Debnath. *Nonlinear Partial Differential Equations for Scientists and Engineers*, Birkhauser Second Edition (2005).
- [2] P.G. Kevrekidis, D.J. Frantzeskakis, and R. Carretero-González. *Emergent Nonlinear Phenomena in Bose-Einstein Condensates: Theory and Experiment*. Springer Series on Atomic, Optical, and Plasma Physics, Vol. **45** (2008).
- [3] G. H. Golub, and J. M. Ortega. *Scientific Computing and Differential Equations An Introduction to Numerical Methods*, Academic Press Second Edition (1992).
- [4] J. C. Strikwerda. *Finite Difference Schemes and Partial Differential Equations*, SIAM Second Edition (2004).
- [5] J. D. Lambert *Numerical Methods for Ordinary Differential Systems*, John Wiley & Sons (1991)
- [6] R. M. Caplan. A Two-Step High Order Compact Scheme for the Laplacian Operator and its Implementation in a Fully Explicit Method for Integrating the Nonlinear Schrödinger Equation. In preparation to be submitted to Appl. Math and Comp., 2011.
- [7] R. M. Caplan. A Simple Modulus-Squared Constant Background Dirichlet Boundary Condition for Time-Dependant Complex Partial Differential Equations and its Application to the Nonlinear Schrödinger Equation. In preparation to be submitted to Appl. Math and Comp., 2011.
- [8] M. S. Ismail. A fourth-order explicit schemes for the coupled nonlinear Schrödinger equation, Appl. Math. and Comp. **196** (2008) 273–284.

- [9] M. M. Cerimele, M. L. Chiofalo, F. Pistella, S. Succi, and M. P. Tosi. Numerical solution of the Gross-Pitaevskii equation using an explicit finite-difference scheme: An application to trapped Bose-Einstein condensates, *Phys. Rev. E.* **62**, 1 (2000) 1382–1389.
- [10] R. Bronson. *Schaum's Outline of Matrix Operations*, McGraw-Hill, First Edition (1988).
- [11] G. H. Golub. *Matrix Computations*, Johns Hopkins University Press, Third Edition (1996).